

# Force Fluctuations in Bead Packs

C.-h. Liu, S. R. Nagel, D. A. Schecter,\* S. N. Coppersmith,†  
S. Majumdar, O. Narayan, T. A. Witten

Experimental observations and numerical simulations of the large force inhomogeneities present in stationary bead packs are presented. Forces much larger than the mean occurred but were exponentially rare. An exactly soluble model reproduced many aspects of the experiments and simulations. In this model, the fluctuations in the force distribution arise because of variations in the contact angles and the constraints imposed by the force balance on each bead in the pile.

Granular materials are ubiquitous, are important to a wide variety of technical processes, and have unusual properties (1). One interesting question is how the stresses in a granular medium are distributed when external forces are applied. Visualizations of two-dimensional (2D) granular systems (2) demonstrate that the weight supported by the particles concentrates into "force chains," and it is natural to expect that similar concentrations of forces will occur in three dimensions. The forces in bead packs give rise to distinctive boundary-layer flow (3); in addition, the propagation of vibrations is acutely sensitive to the specific pattern of contact forces in the pack (4).

Here we present experiments, simulations, and theory characterizing the inhomogeneous forces that occur in stationary three-dimensional (3D) bead packs, focusing particularly on the relative abundance of forces that are much larger than the average. If the bead pack were a perfect lattice, then at any given depth, no forces would be greater than some definite multiple of the average force. At the other extreme, if the network of force-bearing contacts were fractal (5), then fluctuations in the forces (characterized, say, by their variance) would become arbitrarily large as compared with the average force at a given depth, as the system size is increased. Our investigations show that the forces in bead packs are intermediate between these two extremes. The forces are unbounded, but the number of large forces falls off exponentially with the force. The fluctuations re-

main roughly the same as the average force, regardless of how large the bead pack becomes. We will show that a simple model can be used to understand this behavior.

Stress-induced birefringence measurements (2) have visualized the force chains that exist in 2D packings of cylinders arranged in a plane. Placed between two crossed circular polarizers, the cylinders are visible only if they are under pressure and rotate the polarization. Seeing the force inhomogeneities in three dimensions is more difficult, because reflections from bead surfaces will scatter the polarized light into all different polarizations whether the beads are under strain or not. To counter this effect, we have surrounded (6) the beads with an index-matching fluid. The index-matched system does not transmit any light through crossed polarizers unless the beads themselves rotate the polarization. Figure 1 shows an image of a 3D

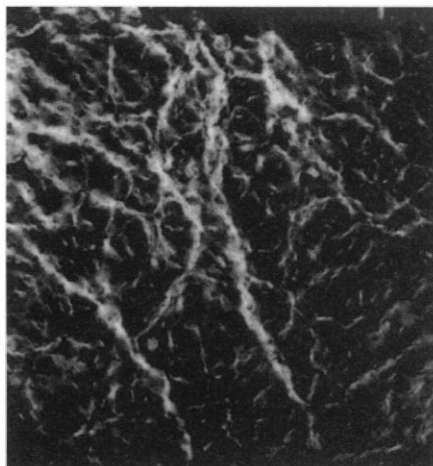


**Fig. 1.** An image of the force chains in a granular medium as viewed between two crossed circular polarizers. The particles, 3-mm Pyrex spheres, are surrounded by an index-matching fluid, a mixture of glycerol and water. The beads are placed in a box with sides 70 mm by 70 mm by 40 mm; the image size is 40 mm by 42 mm. A 200-N force is exerted on a piston that covers the top surface. The stressed beads can be seen as bright regions (the brightness is due to their stress-induced birefringence).

granular material viewed in this manner. The illuminated portions are those where the stresses are greatest. This picture demonstrates that, as in 2D systems, the stress in packed granular materials is concentrated along "chains" and is not distributed uniformly inside the medium.

Although the optical experiment shows that large fluctuations in the forces occur, the force is difficult to calibrate. To obtain the probability,  $P(w)$ , that a bead is subject to a vertical force  $w$ , we used a layer of carbon paper on the inner surface of a container to record the pressure of the beads pressing on that surface (7). The inset to Fig. 2 shows that the area of the mark left by a bead is roughly proportional to  $w$ , the pressure exerted by that bead (that is, the weight supported by it). The main section of Fig. 2 shows the distribution of forces at the bottom surface of a cylindrical container filled with beads, as measured by the marks left on the carbon paper. The circles are the data from the entire base of the container; the squares show the data taken just from the region closest to the cylinder's axis. It is clear that many more strong contacts exist near the cylinder wall than near its axis (8). However, in both cases the data are well described by an exponential function:

$$P(w) = Ce^{-Aw} \quad (1)$$

where the constants  $A$  and  $C$  are given in the legend to Fig. 2. We have performed a numerical simulation of a packing of 500 spherical beads of unit weight and diameter in a uniform gravitational field, interacting with a central force  $F$  of the Hertzian form:  $F = F_0(\delta r)^{3/2}$  where  $\delta r$  is the bead deformation (9). We have calculated the distribution of vertical forces at several different depths  $D$ . Our numerical data indicate that, if one considers the normalized force  $v = w/D$ , the force distribution  $P(v)$  becomes independent of depth for  $D \geq 5$ , and it decays exponentially at large  $v$  (10, 11).

We now propose a simple theoretical model that can be used to understand many of these observations. This model assumes that the dominant physical mechanism leading to force chains is the inhomogeneity of the packing, which causes an unequal distribution of the weights on the beads supporting a given grain. Spatial correlations in these fractions and variations in the coordination numbers of the grains are ignored. We consider a regular lattice of sites, each with a bead of mass unity. The total weight on a given bead is transmitted unevenly to  $N$  adjacent beads in the layer underneath. Specifically, a fraction  $q_{ij}$  of the total weight supported by bead  $i$  in layer  $D$  is transmitted to bead  $j$  in layer  $D + 1$ . Thus, the weight supported by the bead in layer  $D$  at the  $i^{\text{th}}$  site,

C.-h. Liu, Exxon Research and Engineering Company, Route 22 East, Annandale, NJ 08801, USA.

S. R. Nagel, D. A. Schecter, T. A. Witten, James Franck Institute, University of Chicago, 5640 Ellis Avenue, Chicago, IL 60637, USA.

S. N. Coppersmith, AT&T Bell Laboratories, Murray Hill, NJ 07974, USA.

S. Majumdar, Department of Physics, Yale University, New Haven, CT 06511, USA.

O. Narayan, Department of Physics, University of California at Santa Cruz, Santa Cruz, CA 95064, USA.

\*Present address: Department of Physics, University of California, San Diego, La Jolla, CA 92093, USA.

†To whom correspondence should be addressed at: James Franck Institute, University of Chicago, 5640 Ellis Avenue, Chicago, IL 60637, USA.

$w(D, i)$ , satisfies the stochastic equation

$$w(D + 1, j) = 1 + \sum_i q_{ij}(D) w(D, i) \quad (2)$$

We take the fractions  $q_{ij}(D)$  to be random variables, independent except for the constraint

$$\sum_{j=1}^N q_{ij} = 1 \quad (3)$$

The probability of realizing a given set of  $q$ 's at any site  $i$  is given by a distribution function

$$\rho(q_{i1}, \dots, q_{iN}) = \left[ \prod_j f(q_{ij}) \right] \delta\left(\sum_j q_{ij} - 1\right) \quad (4)$$

for some function  $f(x)$ . The "uniform" distribution,  $f(q_{ij}) = \text{constant}$ , is roughly consistent with estimates that we have made by examining the contact angles of the spheres in our simulations (though see below).

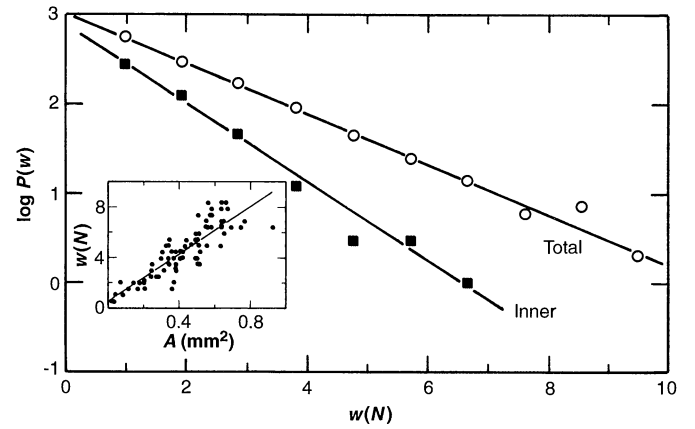
In general, the values of  $w$  at neighboring sites in a given layer are not independent, but one can make a mean field approximation where these correlations are neglected. For the uniform distribution, in terms of the normalized weight variable  $v = w/D$ , as  $D \rightarrow \infty$  the mean field solution for the force distribution  $P_u(v, D)$  is (9):

$$P_u(v) = \frac{N^N}{(N-1)!} v^{(N-1)} e^{-Nv} \quad (5)$$

We have proved for the uniform distribution of  $q$ 's that the mean field approximation yields an exact solution of the model Eq. 2 for all  $N$  (9). This means that for the uniform distribution of  $q$ 's, the distribution of forces per bond on the lattice is exponential, which is the most random distribution that is consistent with the constraint that the sum of the forces is fixed (10–12). Within mean field theory, we have shown that any "generic"  $f(q_{ij})$  gives rise to a  $P(v) \sim v^{N-1} e^{-Nv}$  at large  $v$  (9). Although we do not expect mean field theory to yield an exact force distribution for generic continuous  $f(q)$  functions, we do expect the exact  $P(v)$  to be asymptotically proportional to  $v^{N-1} e^{-Nv}$ . We have checked this numerically for several forms of  $f(q)$  (9).

Figure 3 shows  $P(v)$  calculated by numerical simulation of the "q model" (Eq. 2) with  $f(q) = \text{constant}$  at depth  $D = 1024$  on a periodically continued face-centered-cubic lattice of side 1024, with  $N = 3$  (13). As expected, because the mean field distribution is exact for this case (9), there is excellent agreement with Eq. 5. On the same graph we show  $P(v)$  obtained in the sphere simulation described above. The quantitative agreement between the two is surprisingly good, considering that there is some "arching" (1) in the sphere simulation; a fraction  $\sim 0.06$  of bonds have  $q = 0$ . Within mean field theory, the

**Fig. 2.** The distribution of forces  $P(w)$  versus force  $w$  measured at the bottom of a cylindrical container 90 mm in diameter filled to a height of 75 mm with glass spheres having a radius of 3.5 mm. The bottom of the container was lined with carbon paper, and a force of 310 N was applied to the top surface. The inset shows that the area of a mark on the carbon paper is proportional to the force exerted by the individual bead. In the main panel, the circles show data taken from the entire base of the container; the squares show the data taken only from the region close to the axis (within half of the cylinder's radius). The data are the cumulative results of five separate trials. The lines are exponential fits to the data:  $P(w) = Ce^{-Aw}$  with  $A = 0.64 \text{ N}^{-1}$  and  $C = 988$  for the total and  $A = 1.02 \text{ N}^{-1}$  and  $C = 736$  for the inner region.



large- $v$  exponential decay of  $P(v)$  is not sensitive to the behavior of  $f(q)$  for small  $q$  and hence in three dimensions we expect  $-\log[P(v)] \propto v$  as  $v \rightarrow \infty$  even for distributions with a  $\delta$  function contribution to the  $q$  distribution at  $q = 0$ .

Both the sphere simulation and the  $q$  model have a "hole" in  $P(v)$  at small  $v$ . There is no indication of such a hole in Fig. 2, but if we use the carbon paper it is difficult to resolve the low- $v$  behavior of  $P(v)$ , because beads that support no weight are indistinguishable from vacant spots. However, it is possible that this aspect of

the force distribution is not captured accurately by our model, because the behavior at small  $v$  is more sensitive to the choice of  $q$  distribution.

Neither our simulations nor the  $q$  model of Eq. 2 captures all features of real bead packs. Our simulations include only central forces and ignore friction; the  $q$  model ignores the vector nature of the forces, assuming that only the component along the direction of gravity plays a vital role. The agreement between the different methods provides some indication that the effects that we have neglected do not determine

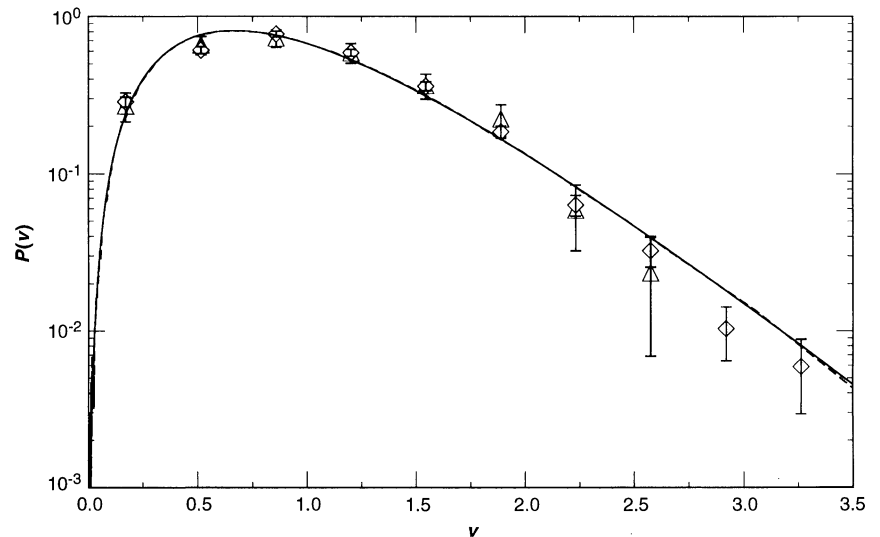


**Fig. 3.** The distribution of forces  $P(v)$  as a function of normalized weight  $v = w/D$  at a given depth  $D$ . Dashed line:  $P(v)$  at  $D = 1024$  obtained by numerical simulation of the model Eq. 2 with  $f(q) = 1$  on a periodically continued face-centered-cubic lattice of transverse extent 1024. Solid line:  $P_u(v)$  obtained from the analytic solution, Eq. 5. The points are  $P(v)$  obtained in the sphere simulation described in the text at depth  $D = 10$  (triangles) and averaged over depths  $D = 6$  through  $D = 13$  (diamonds). There are no adjustable parameters; the scales are set by the normalization requirements

$$\int_0^\infty dv P(v) = 1 \quad \text{and} \quad \int_0^\infty dv v P(v) = 1$$

the main qualitative features of the force distribution at large  $v$ .

Our results indicate that very strong contact forces in bead packs are exponentially rare. We do not know whether such rare fluctuations could account for the heterogeneous phenomena that motivated our study (3, 4), although exponentially uncommon processes are known to dominate certain other stochastic phenomena (14). It is also possible that the large boundary effects apparent in our experiments are intimately connected with the unusual dynamic properties of granular media. Further experiments can address these issues and may provide a new level of understanding of these heterogeneities.

## REFERENCES AND NOTES

1. H. M. Jaeger, J. B. Knight, C.-h. Liu, S. R. Nagel, *Mater. Res. Soc. Bull.* **19**, 25 (1994); H. M. Jaeger and S. R. Nagel, *Science* **255**, 1523 (1992); D. Bideau and A. Hansen, Eds., *Disorder and Granular Media* (North-Holland, Amsterdam, 1993); C. Thornton, Ed., *Powder and Grains* (Balkema, Rotterdam, Netherlands, 1993); A. Mehta, Ed., *Granular Matter* (Springer, Berlin, 1993).
2. P. Dantu, *Ann. Ponts Chaussees* **4**, 144 (1967); A. Drescher and G. de Josselin de Jong, *J. Mech. Phys. Solids* **20**, 337 (1972); T. Travers et al., *Europhys. Lett.* **4**, 329 (1987).
3. S. B. Savage, *Adv. Appl. Mech.* **24**, 289 (1984); R. M. Nedderman, U. Tuzun, S. B. Savage, G. T. Houlsby, *Chem. Eng. Sci.* **37**, 1597 (1982); C. S. Campbell, *Annu. Rev. Fluid Mech.* **22**, 57 (1990).
4. C.-h. Liu and S. R. Nagel, *Phys. Rev. Lett.* **68**, 2301 (1992); *Phys. Rev. B* **48**, 15646 (1993); C.-h. Liu, *ibid.* **50**, 782 (1994).
5. B. Mandelbrot, *The Fractal Geometry of Nature* (Freeman, San Francisco, CA, 1983).
6. T. Wakabayashi, in *Proceedings of the 9th Japan National Congress for Applied Mechanics*, Japan National Committee for Theoretical and Applied Mechanics, Nagoya University, Nagoya, Japan, 29 August to 1 September 1959 (Science Council of Japan, Ueno Park, Tokyo, Japan, 1960), pp. 133–140; A. Drescher, *Geotechnique* **26**, 591 (1976). These studies did not visualize the individual stress lines in a 3D system.
7. H. Kuno and I. Kuri, *Powder Technol.* **34**, 87 (1983).
8. Analogous boundary effects in free-standing piles have been explored by J.-P. Bouchaud, in *Non-linearity and Breakdown in Soft Condensed Matter*, Lecture Notes in Physics 437, K. Bardhan et al., Eds. (Springer, Berlin, 1994), pp. 47–53; J.-P. Bouchaud, M. Cates, Ph. Claudin, unpublished data.
9. S. N. Coppersmith, C.-h. Liu, S. Majumdar, O. Narayan, T. Witten, unpublished data.
10. Earlier simulations have yielded results consistent with an exponential distribution of contact forces: P. A. Cundall, J. T. Jenkins, I. Ishibashi, in *Powders and Grains*, J. Biarez and R. Gourves, Eds. (Balkema, Rotterdam, Netherlands, 1989), pp. 319–322; J. T. Jenkins, P. A. Cundall, I. Ishibashi, *ibid.*, pp. 257–274; K. Bagi, in *Powders and Grains*, C. Thornton, Ed. (Balkema, Rotterdam, Netherlands, 1993), pp. 117–121.
11. A. Pavlovitch, unpublished data.
12. A. Katz, *Principles of Statistical Mechanics: The Information Theory Approach* (Freeman, San Francisco, CA, 1967); L. Rothenburg, thesis, Carlton University, Ottawa, Canada (1980).
13. Within our approximation of placing the grains on a uniform lattice, the reasonable choice for  $N$  is the dimensionality ( $d$ ) of the system: For  $d = 3$  a 3D system, the grains are approximated as being in triangular lattice layers on a face-centered-cubic lattice.
14. P. M. Duxbury and P. L. Leath, *Phys. Rev. Lett.* **72**, 1805 (1994) and references therein.
15. We thank R. Behringer for showing us his birefringence experiments and H. Jaeger, J. Knight, and A. Pavlovitch for many important discussions and for providing us with (11) in advance of publication. The work of O.N. was supported by the Society of Fellows at Harvard University and the Institute for Theoretical Physics at Santa Barbara (NSF grant PHY89-04035). S.N.C. acknowledges hospitality

as a Materials Research Laboratory visitor at the University of Chicago. Supported in part by the Materials Research Science and Engineering Center Program of NSF under awards DMR-8819860 and DMR-9400379.

17 January 1995; accepted 31 May 1995

## Total Alignment of Calcite at Acidic Polydiacetylene Films: Cooperativity at the Organic-Inorganic Interface

Amir Berman, Dong June Ahn, Anna Lio, Miquel Salmeron, Anke Reichert, Deborah Charych\*

Biological matrices can direct the absolute alignment of inorganic crystals such as calcite. Cooperative effects at an organic-inorganic interface resulted in similar co-alignment of calcite at polymeric Langmuir-Schaefer films of 10,12-pentacosadiynoic acid (p-PDA). The films nucleated calcite at the (012) face, and the crystals were co-aligned with respect to the polymer's conjugated backbone. At the same time, the p-PDA alkyl side chains reorganized to optimize the stereochemical fit to the calcite structure, as visualized by changes in the optical spectrum of the polymer. These results indicate the kinds of interactions that may occur in biological systems where large arrays of crystals are co-aligned.

Biological organisms are capable of controlling inorganic crystal growth to a remarkable degree (1, 2). This exquisite control is usually achieved with the use of an organic polymeric "matrix" of highly acidic macromolecules. In certain cases, the minerals that are formed by biological organisms are uniquely oriented or co-aligned relative to the organic matrix (3). The in vitro synthesis of novel organic-inorganic composites with properties analogous to those produced by Nature continues to challenge the materials scientist. The use of simplified surfactant molecular assemblies (4, 5) resembling biological membranes (for example, monolayers, multilayers, or vesicles) is one approach toward achieving this goal. These structures provide modifiable interfacial functionalization and well-defined spatial organization. A number of elegant examples demonstrate the nucleation and growth of organic (6) and inorganic crystals at monolayer assemblies (7–9). To our knowledge, the crystals produced by these methods are oriented only in the direction normal to the membrane plane (8, 9). The crystal axes in the plane of nucleation do not appear to be aligned with a structural parameter of the nucleation surface.

Previous studies have indicated that stereochemical match between the organic and inorganic interfaces is a predominant

factor in determining the specific nucleation face type, in addition to lattice match and electrostatic interactions (10–12). One difficulty is that structural information regarding the organic template has so far been obtained in the absence of mineralization at the monolayer [for example, from grazing incidence x-ray diffraction, electron diffraction, and x-ray reflectivity (13, 14)], yielding the average spacing between organic functional groups and the two-dimensional unit cell dimensions. Furthermore, it has been suggested that synergistic changes in the organic template structure occur upon interaction with solid interfaces, as is the case when crystals are forming at the hydrophilic head-group region (12). In such cases, in situ structural information regarding the organic template is even more elusive as dynamic changes in monolayer organization may occur.

In this report, we demonstrate that cooperativity at the organic-inorganic interface can result in complete alignment of calcite crystals along an identifiable structural feature of the acidic p-PDA matrix. Lattice match between calcite and p-PDA dominates along the  $a$  axis of the calcite crystal. Symmetry reduction in the p-PDA template coupled with proper stereochemical match ultimately controls the co-alignment of the crystals and determines the nucleation face type. Structural reorientation of the p-PDA matrix occurs upon calcite mineralization to optimize the stereochemical fit. The reorientation is readily observed in p-PDA as a blue-to-red chro-

Center for Advanced Materials, Lawrence Berkeley Laboratory, Berkeley, CA 94720, USA.

\*To whom correspondence should be addressed.